MATEC Web of Conferences **165**, 22016 (2018) https://doi.org/10.1051/matecconf/201816522016
FATIGUE 2018

Thermo-mechanical fatigue prediction of a steam turbine shaft

Martin Nesládek[1,*], *Michal* Bartošák[1], *Josef* Jurenka[1], *Jan* Papuga[1], *Milan* Růžička[1], *Petr* Měšťánek[2] and *Jan* Džugan[3]

[1]Czech Technical University in Prague, Faculty of Mechanical Engineering, Technická 4, 166 07 Prague 6, Czech Republic
[2]Doosan Škoda Power s.r.o., Tylova 1/57, 301 28 Plzeň, Czech Republic
[3]COMTES FHT a.s., Průmyslová 995, 334 41 Dobřany, Czech Republic

Abstract. The increasing demands on the flexibility of steam turbines due to the use of renewable energy sources substantially alters the fatigue strength requirements of components of these devices. This paper presents Thermo-Mechanical Fatigue (TMF) design calculations for the steam turbine shaft. The steam turbine shaft is exposed to complex thermo-mechanical loading conditions during the operating cycle of the turbine. An elastic-plastic structural Finite Element Analysis (FEA) of the turbine shaft is performed for the turbine operating cycle on the basis of calculated temperature fields obtained in a previous transient thermal FEA. The temperature dependent material parameters, which are used in the elastic-plastic FEA, are obtained from the uniaxial tests. Consequently, the TMF is predicted for the steam turbine shaft. Several fatigue criteria are used for the identifications of the critical domain and for the TMF damage assessment of the turbine shaft.

1 Introduction

The energy industry has been experiencing significant changes recently. The overall share of renewable sources in the Czech Republic is around 13 percent. In Germany it is even more, approximately 30 percent and the trend is that this share will continue to grow significantly in the future. However, instability of the power output due to these sources may cause problems in energy supplies if it is not compensated by some back-up sources. Currently, there are no reliable ways to save energy for power shortages in the network in such a large scale. This role must be taken over by traditional thermal power sources such as gas-fired power plants. The problem is that these plants already have to or will have to cover shortages in the daily regime. Increased number of start-ups and shutdowns as long as increasing demands on speed-up of the start-ups set new challenges in the gas and steam turbine design.

Components of steam turbines are often exposed to thermo-mechanical loading due to variable loading conditions, including start-up, full load, load change and stop phases. There have been increasing demands for reliable Low-Cycle Fatigue (LCF) and TMF fatigue predictions [1-3] of components, in order to provide safety, guaranteed function, durability and in order to avoid over-dimensioning of the components. The main damage mechanisms of TMF are often referred to as oxidation, fatigue and creep [4, 5]. Constitutive material model derived from the material testing, finite element analysis and suitable fatigue criterion is required for the reliable damage assessment of components subjected to cyclic thermo-mechanical loading conditions [3].

The Flexturbine project aims to revise the design of key turbine components and propose new design methodologies so that the turbines can cope with the changing situation in the transmission grids. The paper illustrates the work done on the prediction methodology for thermo-mechanical fatigue design of steam turbine shafts. The fatigue damage is assessed for the turbine shaft on the basis of several fatigue criteria. The turbine shaft is exposed to complex thermo-mechanical loading due to variable service conditions.

The paper presents experimental results of the uniaxial material tests. The temperature dependent constitutive material model is calibrated on the basis of the obtained experimental data. The material model is elastic-plastic and is used in the structural FEA of the steam turbine shaft, which is performed on the basis of the simulated temperature fields that are obtained from the previous transient thermal FEA. The finite element calculations for the steam turbine shaft are performed in the commercial finite element software ANSYS. Consequently, TMF is predicted for the turbine shaft on the basis of the calculated stress, strain and temperature histories.

The first fatigue criterion used for the TMF life prediction of the turbine shaft is the Damage Operator Approach (DOA) [6, 7]. The DOA is based on the classical strain-life approach. Cycle equivalent temperature or separated rain-flow counting are no longer required with the DOA. The oxidation effect is taken into account indirectly, because experiments were carried out under ambient conditions. The mean-stress effect is taken into account in the DOA as well, and is represented by the Smith, Watson and Topper damage parameter. The other fatigue criteria are the uniaxial

* Corresponding author: martin.nesladek@fs.cvut.cz

SWT [8] and Nihei [9] methods. The classical SWT fatigue damage model is often used in the energy industry. However, the original SWT and the Nihei criteria are not formulated to handle the loading cycles with variable temperatures. An appropriate cycle reference temperature has to be selected if these methods are to be applied. All the applied methods are based on the standard isothermal low-cycle fatigue data, i.e. strain-life curves obtained under isothermal loading conditions. From a practical point of view, the prediction models are implemented as the in-house codes (C++ and APDL scripts). The TMF results obtained for the steam turbine shaft with the DOA, the SWT and the Nihei models are compared.

2 The material

2.1. Experimental data

The steam turbine shaft usually operates under a wide temperature range. If accurate material response calculation and fatigue prediction are to be performed, the temperature dependence of the respective material model parameters must be known. The experiments should be carried out in such a way that the exhibited temperature range of the investigated component is fully covered. The investigated material of the steam turbine shaft is chrome-molybdenum creep resistant steel. The following uniaxial tests were conducted in order to identify temperature dependent material behaviour:

- Static tensile tests,
- Low-cycle fatigue tests.

The uniaxial tests were performed under ambient isothermal loading conditions in the temperature range of 20 to 600 °C. The low-cycle fatigue tests were performed on the servo-hydraulic MTS 810 machine. The split furnace Mellen was used for the heating of the specimens. The force was measured by the load cell. The LCF tests were performed as fully reversed at high strain rates and as strain controlled. High temperature extensometer with ceramic rods was used for the strain control. The tensile and the LCF tests were performed for the cylindrical specimens.

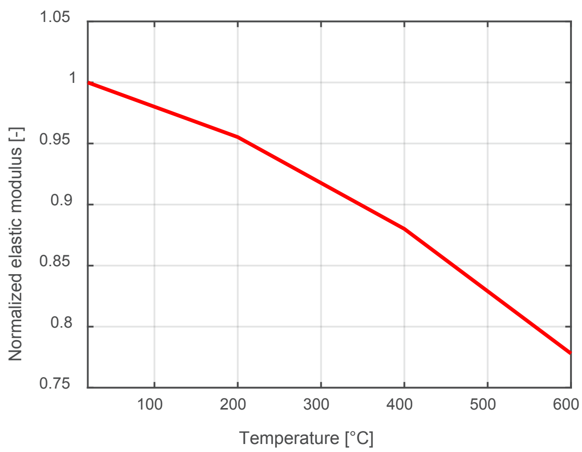

Fig. 1. The temperature dependent elastic modulus.

The temperature dependent elastic modulus E, the Cyclic Stress-Strain Curves (CSSC), and the Manson-Coffin and the Basquin fatigue curves were derived from the low-cycle fatigue tests. The CSSC constitutes the material stress-strain response under cyclic loading and has the following mathematical form, known as the Ramberg-Osgood relation:

$$\varepsilon_a = \frac{\sigma_a}{E} + \left(\frac{\sigma_a}{K'}\right)^{1/n'}, \quad (1)$$

where ε_a and σ_a are the strain and stress amplitudes, respectively. K' is the cyclic hardening coefficient and n' is the cyclic strain-hardening exponent. The CSSS were obtained from the stabilized hysteresis loops at mid-life.

The Manson, Coffin and Basquin curves are often necessary for the damage assessment for the LCF and the TMF loading conditions. The Manson, Coffin and Basquin curves are written in the common mathematical form as follows:

$$\varepsilon_a = \frac{\sigma_f'}{E}\left(2N_f\right)^b + \varepsilon_f'\left(2N_f\right)^c, \quad (2)$$

where N_f is the number of cycles to failure, σ_f' and b are the fatigue strength coefficient and exponent, respectively. ε_f' is the fatigue ductility coefficient and c is the fatigue ductility exponent. The number of cycles to failure was determined in a classical way, when 10% drop of the tensile stress occurred in comparison with the stabilized state. The parameters of the Manson, Coffin and Basquin curves are temperature dependent.

Fig. 2. The temperature dependent cyclically stable cyclic

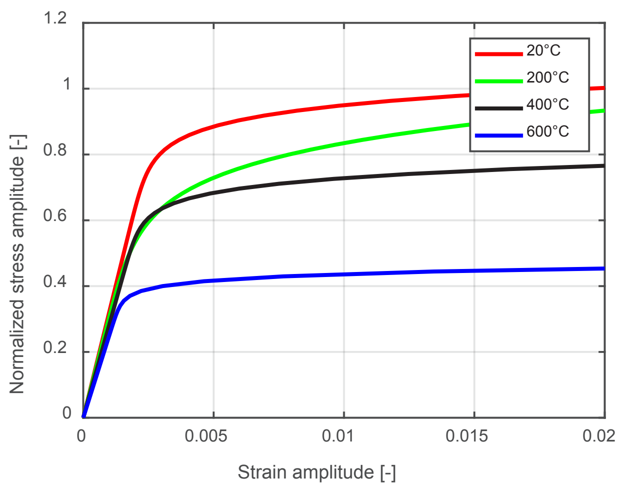

stress-strain curves.

The temperature dependent elastic-modulus for the investigated material is presented in Fig.1. The elastic modulus was determined from the stabilized hysteresis loops at mid-life. The CSSC for the selected temperatures are presented in Fig.2. The Manson, Coffin and Basquin curves are presented in Fig. 3. The specimens showed monotonically increasing durability as well as the ductility for the high strain ranges with the increasing temperature.

In our future work, the experimental data will be extended with low-cycle fatigue tests with hold time in a tension. The obtained experimental results are consequently used for the selected constitutive material model calibration.

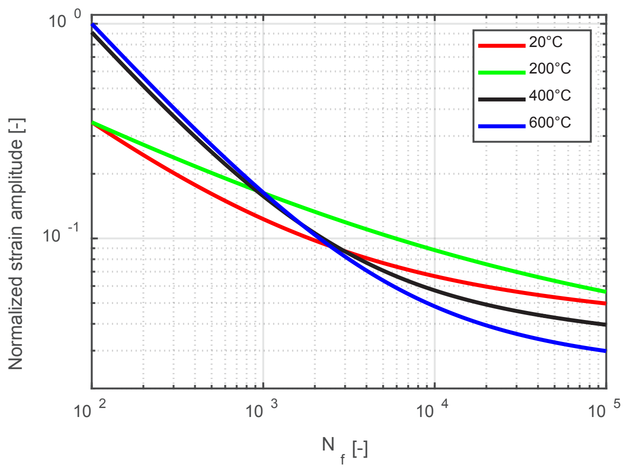

Fig. 3. The temperature dependent Manson, Coffin and Basquin curves.

2.2 Constitutive material model

A constitutive material model must be able to describe the cyclic material behaviour for the temperature range of the steam turbine shaft that is exhibited. The temperature-dependent Chaboche non-linear kinematic hardening model [10, 11] is selected for the elastic-plastic FEA.

The stress tensor $\boldsymbol{\sigma}$ is obtained on the basis of the generalized Hooke law, as follows:

$$\boldsymbol{\sigma} = \mathbf{C}:(\boldsymbol{\varepsilon} - \boldsymbol{\varepsilon}_p - \boldsymbol{\varepsilon}_{th}), \tag{3}$$

where $\boldsymbol{\varepsilon}$ is the total strain tensor, $\boldsymbol{\varepsilon}_{\mathrm{th}}$ is the thermal strain tensor, and $\boldsymbol{\varepsilon}_{\mathrm{p}}$ is the plastic strain rate tensor. $\mathbf{C}$ denotes the fourth order isotropic elastic tensor. The elastic tensor components are defined by the temperature-dependent elastic modulus E, and by the Poisson ratio v.

The model assumes associated plastic flow:

$$\dot{\boldsymbol{\varepsilon}}_p = \dot{\bar{\varepsilon}}_{\mathrm{p}} \frac{\partial f(\boldsymbol{\sigma}-\boldsymbol{\alpha})}{\partial \boldsymbol{\sigma}}, \tag{4}$$

where $\dot{\boldsymbol{\varepsilon}}_p$ represents the plastic strain rate tensor, and $\dot{\bar{\varepsilon}}_{\mathrm{p}}$ is the equivalent plastic strain rate, defined as:

$$\dot{\bar{\varepsilon}}_{\mathrm{p}} = \sqrt{\frac{2}{3}\dot{\boldsymbol{\varepsilon}}_p:\dot{\boldsymbol{\varepsilon}}_p}. \tag{5}$$

The pressure-independent von Mises yield function, allowing for kinematic hardening, is defined as:

$$f(\boldsymbol{\sigma} - \boldsymbol{\alpha}) = k, \tag{6}$$

where k is the material dependent and the temperature dependent yield stress, and $f(\boldsymbol{\sigma} - \boldsymbol{\alpha})$ denotes the equivalent Mises stress with respect to the backstress $\boldsymbol{\alpha}$, defined as:

$$f(\boldsymbol{\sigma} - \boldsymbol{\alpha}) = \sqrt{\frac{2}{3}(\mathbf{S} - \boldsymbol{\alpha}'):(\mathbf{S} - \boldsymbol{\alpha}')}, \tag{7}$$

where $\mathbf{S}$ denotes the deviatoric stress tensor, and $\boldsymbol{\alpha}'$ is the deviatoric part of the backstress. Assuming the non-linear kinematic hardening model, the overall backstress is composed of multiple backstress components as follows:

$$\boldsymbol{\alpha} = \sum_{k}^{3} \boldsymbol{\alpha}_{\mathrm{k}}. \tag{8}$$

The non-isothermal evolution law of the backstress component is defined as:

$$\dot{\boldsymbol{\alpha}}_{\mathbf{k}} = \frac{2}{3} C_k \dot{\boldsymbol{\varepsilon}}_p - \gamma_k \boldsymbol{\alpha}_{\mathrm{k}} \dot{\bar{\varepsilon}}_{\mathrm{p}} + \frac{1}{C_k}\frac{\partial C_k}{\partial T} \boldsymbol{\alpha}_{\mathrm{k}} \dot{T}, \tag{9}$$

where C_k and γ_k are temperature dependent material parameters. The model with three backstresses is selected. γ_3 is considered as a constant, and is equal to zero. Ratcheting is not studied in this paper.

In this study, the temperature dependent parameters k, C_k and γ_k were obtained by the standard least-square method from the LCF test data for each test temperature indepedently, and by interpolation for the temperatures between the test temperatures.

3 Fatigue damage assessment

3.1 Fatigue damage calculation concept

Damage calculation forms a part of post-processing, and is based on the results of previous mechanical FEA. The following fatigue criteria are applied in order to predict the lifetime for the steam turbine shaft:

- The Damage Operator Approach (DOA also known as the Nagode method)
- The SWT method
- The Nihei method

From a practical point of view, the fatigue criteria were implemented as post-processing code. The APDL script intended especially for finding the critical domain in the turbine shaft was coded. A user can choose from a wide range of possible approaches – the maximum or range of the stress or strain tensor components, the stress or strain tensor invariants or the Manson-McKnight method. The selected criterion is evaluated in the corner nodes of the element set, which needs to be first predefined in the turbine shaft FE model in ANSYS.

The script creates several types of the outputs. First, the text file with the node numbers that are sorted according to the value of the criterion that is written. The criterion value and time when maximum and minimum occur are also recorded. A separate APDL script may then be applied to upload the obtained results into the original **.rst* file. Second, for the individual nodes from the selected element set, separate data files containing time histories of the stress and the strain components and the temperatures are written. Then, these files are used for the fatigue analysis using the Nagode, SWT or the

 https://doi.org/10.1051/matecconf/201816522016

Nihei method, which are implemented in *C*++ code. The results expressed as the local fatigue damage and the lifetime are stored in the separate text file, which is then used for the data upload back into the source file **.rst*. As well as the data obtained by the APDL script, these results are mapped on the FE model of the turbine shaft and could be visualised in ANSYS, for instance, as contour plots. The above mentioned conception of the program codes for the fatigue prediction of the turbine shaft is represented by the flowchart in Fig. 4.

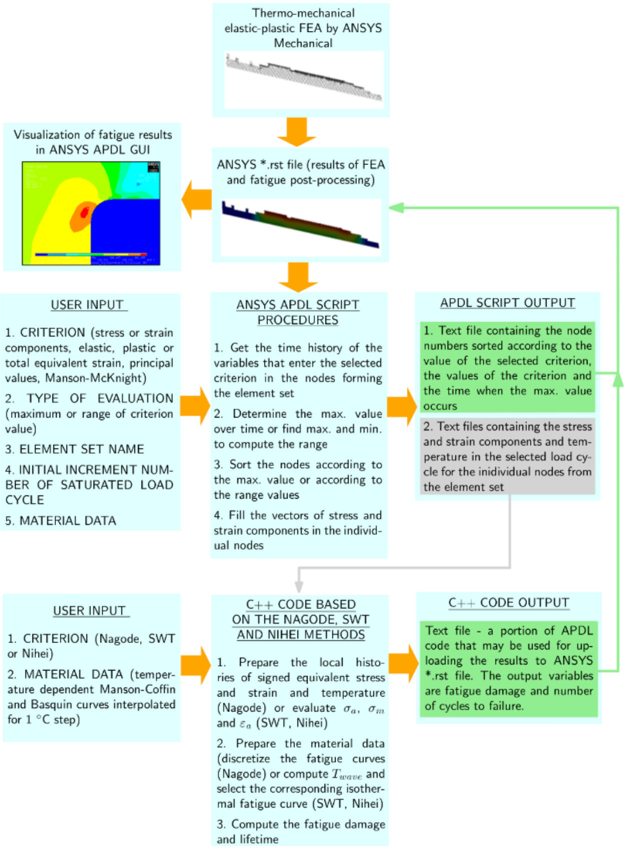

Fig. 4. The basic conception of the developed software codes for the fatigue prediction of the steam turbine shafts.

3.2 The SWT and the Nihei methods

To take the influence of variable stress and strain into account in fatigue prediction the following parameter is widely used:

$$P_{SWT} = \sqrt{E\varepsilon_a(\sigma_a + \sigma_m)}, \tag{10}$$

which is the well-known SWT parameter [8]. E is the Young's modulus, ε_a is the total mechanical strain amplitude and σ_a and σ_m is the stress amplitude and mean, respectively.

By considering the Walker mean stress correction, Nihei et al. 9 have introduced a modification of the original SWT formula in this form:

$$P_{Nih} = \sqrt{\sigma_a^w(\sigma_a + \sigma_m)^{1-w}\varepsilon_a E}. \tag{11}$$

Recommended value for the w exponent is 0.5. Evaluation of the stress and strain amplitudes may be done according to the Manson-McKnight method [12] by evaluating means and amplitudes of the individual stress or strain tensor components separately. For the stress tensor components we may write

$$\sigma_{ij,a} = \frac{max_t(\sigma_{ij}) - min_t(\sigma_{ij})}{2}, \tag{12}$$

$$\sigma_{ij,m} = \frac{max_t(\sigma_{ij}) + min_t(\sigma_{ij})}{2}. \tag{13}$$

The equivalent stress amplitude and mean is then computed by considering the von Mises norm:

$$\sigma_a = \frac{\sqrt{2}}{2}\sqrt{\begin{array}{c}(\sigma_{xx,a} - \sigma_{yy,a})^2 + (\sigma_{yy,a} - \sigma_{zz,a})^2 + \\ +(\sigma_{xx,a} - \sigma_{zz,a})^2 + \\ +6(\sigma_{xy,a}^2 + \sigma_{xz,a}^2 + \sigma_{yz,a}^2)\end{array}} \tag{14}$$

and

$$\sigma_m = \frac{\sqrt{2}}{2}\sqrt{\begin{array}{c}(\sigma_{xx,m} - \sigma_{yy,m})^2 + (\sigma_{yy,m} - \sigma_{zz,m})^2 + \\ +(\sigma_{xx,m} - \sigma_{zz,m})^2 + \\ +6(\sigma_{xy,m}^2 + \sigma_{xz,m}^2 + \sigma_{yz,m}^2)\end{array}} \tag{15}$$

The equivalent mean stress value σ_m is signed according to the sign of the maximum principal stress over the entire analysed time history.

The resulting value of fatigue lifetime obtained by these methods depends on the local load history represented by the parameter P on the one hand and on the material fatigue properties involved by the Manson-Coffin and Basquin parameters of regression $\sigma_f', b, \varepsilon_f', c$ on the other hand. However, these parameters are temperature dependent, which in case of thermo-mechanical loading sets additional requirements on the computational procedure - a decision process that determines the local reference temperature over the entire cycle has to be implemented. For this purpose, selection of the local reference temperature is based on the time-weighted average over the assumed cycle.

3.3 The Damage Operator Approach

The DOA is used for continuous fatigue damage calculations of the steam turbine shaft. The DOA and is an extension of the strain-life approach to loading cycles with variable amplitude and temperature. There is no longer a need for cycle equivalent temperature and separate rain-flow cycle counting [6].

The stress tensors from structural FEA are transferred into the equivalent stress histories by applying different multiaxial criteria. The signed von Mises equivalent stress, or the critical plane approach are frequently used with the DOA. In this study, the signed von Mises equivalent stress is selected for the steam turbine shaft.

In this paper the temperature histories, $T_i(t_i)$, the signed von Mises equivalent stress histories, $\sigma_i(t_i)$, and as well the equivalent mechanical strain histories, $\varepsilon_i(t_i)$, are obtained from the previous structural FEA of the steam turbine shaft.

The constitutive material model used in the structural FEA of the steam turbine shaft is elastic-plastic, therefore the equivalent mechanical strain, $\varepsilon_i(t_i)$, is the elastic-plastic strain, $\varepsilon^{ep}(t_i)$, that contributes to the fatigue damage, as follows:

$$\varepsilon^{ep}(t_i) = \varepsilon_i(t_i). \tag{16}$$

Next, the equivalent stress, $\sigma_i(t_i)$, and the elastic-plastic strain, $\varepsilon^{ep}(t_i)$, are transferred into the selected damage parameter $P(t_i)$. If no mean-stress correction is used, then:

$$P(t_i) = \varepsilon^{ep}(t_i). \tag{17}$$

In this paper, the mean stress effect is included in the Smith-Watson-Topper damage parameter, which is defined as:

$$P_{SWT}(t_i) = \sqrt{(\sigma_m(t_i) + \sigma_a(t_i))E(T_i)\varepsilon_a^{ep}(t_i)}, \tag{18}$$

where $E(T_i)$ is the temperature dependent instantaneous elastic modulus. The SWT damage parameter used in the DOA requires online calculation of the mean stress, $\sigma_m(t_i)$, and the stress amplitude, $\sigma_a(t_i)$, and also the strain amplitude $\varepsilon_a{}^{ep}(t_i)$ [11].

The fatigue damage $D_f(t_i)$ can be expressed as the total variation, as follows:

$$D_f(t_i) = D_f(t_{i-1}) + |\mathcal{D}(t_i) - \mathcal{D}(t_{i-1})|. \tag{19}$$

$\mathcal{D}(t_i)$ is the damage operator. The damage operator introduces the cyclic damage evolution and follows the Masing and memory rules. The damage operator is expressed as:

$$\mathcal{D}(t_i) = \sum_{j=1}^{n_p} \mathcal{D}_j(t_i) = \sum_{j=1}^{n_p} \gamma_j(T_i)\, P_{\gamma j}(t_i) \tag{20}$$

for $0 \le t_1 \le t_2 \le ... \le t_i \le ...$, where $P_{\gamma j}(t_i)$ is the play operator with a general initial value given as:

$$P_{\gamma j}(t_i) = max\left\{P(t_i) - p_j\ , min\left\{P(t_i) + +p_j\ , \frac{\gamma_j(T_{i-1})}{\gamma_j(T_i)}\ P_{\gamma j}(t_{i-1})\right\}\right\}. \tag{21}$$

$P_{\gamma j}(t_i)$ represents the backstress and follows kinematic hardening. p_j are the yield stresses of the segment sliders. $\gamma_j(T_k)$ are the temperature-dependent Prandtl densities, and can be obtained explicitly as follows:

$$\gamma_j(T_k) = \frac{1}{p_{j+1} - p_j}\left(\frac{d_{f\,j+1}(T_k)}{4} - -\sum_{i=1}^{j-1} \gamma_j(T_k)(p_{j+1} - p_j)\right). \tag{22}$$

$\gamma_j(T_k)$ are obtained from the temperature dependent strain-life curves, Fig.3, or from a damage parameter - life curves, which need to have been transformed previously from the P-N_f curves to the corresponding P-d_f curves. d_f is a damage of one cycle, obtained as follows:

$$d_f = \frac{1}{N_f}. \tag{23}$$

The fatigue damage is modelled with the intensive use of the hysteresis operators. The DOA is a continuous rain-flow method for cycles with variable temperature [13].

Assuming a doubled equivalent stress, strain and temperature history, the predicted number of cycles to failure for a selected damage parameter is calculated as follows [7]:

$$N_f = \frac{1 - D_1 + D_2}{D_2}, \tag{24}$$

where D_1 is the fatigue damage of the first run, and D_2 is the fatigue damage of the subsequent run. The limit damage value is assumed to be equal to 1. If $D_1 \ge 1$ then $N_f = 1$.

It should be remarked that the stresses obtained from the elastic-plastic FEA should relax. The real material behaviour is viscoplastic. In our future work, the viscoplastic approximation will be used [7]. The fatigue damage model will be extended with a creep damage model. With the DOA, creep and fatigue damage calculations are separated and the oxidation effect is taken into account indirectly [6]. The DOA is suitable for the engineering TMF calculations and for the complex stress, strain and temperature histories.

4 Finite element analysis of the steam turbine shaft

The overall objective of the finite element analyses (FEAs) was to suggest a reliable and effective way how to perform simulations of the elastic-plastic material behaviour in the critical domains of turbine shafts with respect to the complex operating modes. A model case of the turbine shaft was selected and all calculations as part of the development of the methodology were done on this component.

Heat resulting from dissipative processes in material is negligible in comparison with convective heat. Therefore sequential heat transfer-stress analysis was used to calculate mechanical response. The temperature fields obtained from the transient thermal analysis of the steam turbine shaft are subsequently used in the elastic-plastic FEA of the shaft.

The assumption of axisymmetry of the shaft geometry and loads is adopted for the finite element (FE) model. The following types of loads are considered as dominant and therefore applied in the model:

- Thermal loads caused by the constrained thermal expansion
- Inertia loads due to rotating mass of the shaft and blades
- Loads due to the steam flow impact

In this study, the time distribution of the loads representing the turbine cold-start process is assumed. The steam turbine cold-start procedure consists of several phases. During the pre-warming phase the turbine is rotated by a turning gear while being heated by warming steam. The acceleration phase consists of controlled increase of the speed of rotation to its nominal value in vacuum conditions. Loading phase is then a sequence of several controlled steps, during which the steam mass flow, temperature and pressure reach their nominal characteristics. After this initial set of load regimes, the turbine operates in approximately steady inlet and outlet conditions and the rotor temperature field reaches its steady state. The shutdown procedure is

 https://doi.org/10.1051/matecconf/201816522016

divided into three phases: unloading to 50% and run-out, during which the speed of rotation goes from maximum to zero, and cooling in the final stage. Due to the casing insulation, it may take several weeks to cool down the turbine to the initial state.

The thermal response of the shaft material is simulated by the sequence of ten separate transient thermal analyses defined in the ANSYS Mechanical FE code. In general, convective heat transfer conditions are defined as couples of the heat transfer coefficient values and steam temperatures. Moreover, the blade roots are also considered in the model for accurate determination of the temperature field in the vicinity of the blade grooves (Fig. 5).

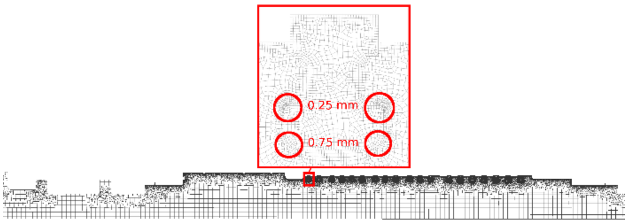

Fig. 5. The finite element model mesh. The element size in the blade grooves is illustrated.

Mechanical response of the material is analysed by taking the calculated temperature fields within the ten individual load regimes into account. Frictional contacts are set between the blade roots and grooves and the inertial forces due to rotating blade aerofoils are replaced by concentrated forces in the aerofoil centroids. The steam flow effect is replaced by the horizontal force component acting in the centroids as well.

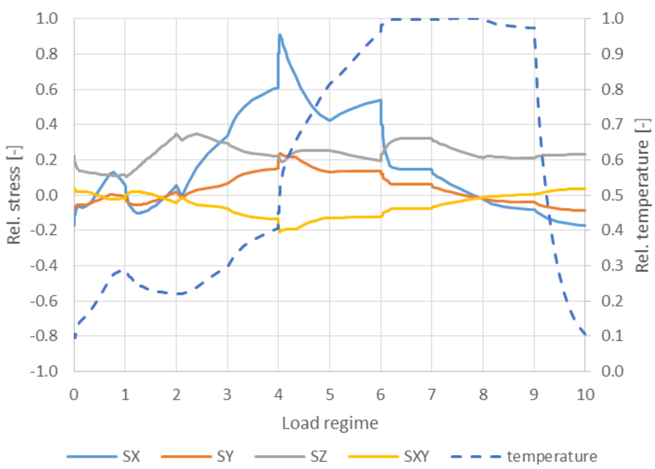

Fig. 6. Sample local stress and temperature history.

To obtain the saturated stress-strain response of the steam turbine shaft, three cold-start cycles were analysed consecutively. The dominant stress component in the potentially critical domains is the normal stress in the radial direction, and is presented in Fig. 6. It occurs in a particular time instant during the start-up when the maximum speed of rotation is reached while the material is not yet fully warmed up.

5 Fatigue damage assessment for the steam turbine shaft

For the purpose of this study, the fatigue prediction is focused on the critical site detection and on the assessment of the thermo-mechanically induced fatigue damage evaluated by the three methods. The FE model loaded by the set of loads as mentioned in the previous section was analysed. The fatigue analysis was done by using the SWT and the Nihei methods, as well as the DOA by Nagode et al. The work and the results published here extend and refine those presented in [14].

Based on the results of the FE simulations and the overall expertise, potentially critical domains were defined (Fig. 7). These domains are primarily the regions of the blade grooves and the main internal seals. The element set spanning these domains was defined for the purpose of performing fatigue analysis using the in-house codes. Fig. 8 to Fig. 10 show the fatigue damage contours evaluated by the mentioned criteria in the domain, which is framed in red in Fig. 7.

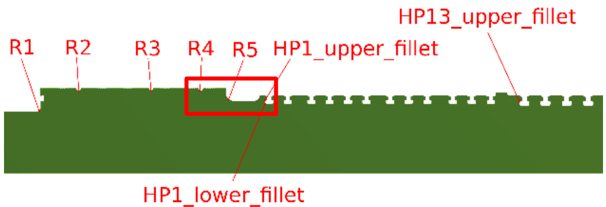

Fig. 7. The potential critical domains for the steam turbine shaft.

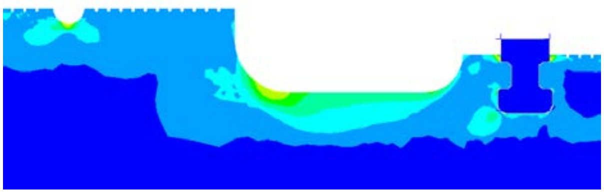

Fig. 8. Distribution of the fatigue damage computed by the DOA.

Fig. 9. Distribution of the fatigue damage computed by the SWT method.

Fig. 10. Distribution of the fatigue damage computed by the Nihei method.

in the main internal sealing. Predicted life of this place is 2600 cold-start cycles. It is also the place of the maximum equivalent mechanical strain range. The Nihei and the SWT methods predict critical site in the "R1" domain, however the predicted life is two orders of magnitude higher than in the case of the DOA results. This observation reveals the expected weakness of the two isothermal methods, which is the nonrigorous approach to selecting the cycle reference temperature.

	R1	R2	R3	R4	R5	HP1_upper_fillet	HP1_lower_fillet	HP13_upper_fillet
N by Nagode [-]	5.3E+04	2.1E+04	2.6E+03	5.7E+03	6.2E+03	4.3E+04	6.9E+03	7.3E+04
N by SWT [-]	1.3E+06	5.9E+07	5.8E+06	4.4E+07	5.7E+08	8.6E+11	3.0E+06	1.8E+08
N by Nihei [-]	1.7E+06	1.1E+08	1.1E+07	8.6E+07	1.2E+09	3.4E+12	4.3E+06	1.5E+09

Table 1. Results of fatigue analysis in the selected domains of the turbine shaft.

Table 1 provides the numerical results in terms of the fatigue life values in the selected domains. The most critical place according to the DOA is the "R3" domain

It should be noted that the presented results are preliminary and will be further refined based on the progress of experimental programme conducted to determine the material behaviour especially with focus on the viscoplastic response.

6 Conclusions

The work done within the Flexturbine project was introduced in this paper, and some results concerning the fatigue prediction methodology applicable to steam turbine rotors were presented. The strategy for TMF prediction of this structure is based on 2D axisymmetric FE model for simulating the time variable thermo-mechanical stress-strain response. The in-house codes for fatigue analysis that are capable of processing the ANSYS **.rst* files are based on a number of criteria, including the Manson-McKnight, the DOA and other methods. It is possible to determine the critical domain including the extent of the damage or the number of cycles to initiation. The obtained results can be mapped to the original FE model to obtain an overview of the distribution of the resulting values.

The used elastic-plastic material with kinematic hardening is capable of describing temperature dependent cyclic plasticity, but cannot capture time dependent material behaviour. However, the advantage of the elastic-plastic material model is computational speed in comparison with viscoplastic material models.

The advantage of the DOA is that the approach uses only isothermal data that are easy to obtain. The continuous fatigue damage calculation is convenient for the complex thermo-mechanical loading cycles as in the case of the steam turbine shaft.

In our future work, the viscoplastic approximation will be used for the elastic-plastic FEA results of the steam turbine shaft. For that reason, the LCF tests will be extended with LCF tests with a hold time. The DOA results for the signed von Mises equivalent stress will be compared with results obtained with the critical plane approach. A creep damage model will be added to the fatigue damage.

Acknowledgement: This project has received funding from the European Union's Horizon 2020 research and innovation programme under the Grant Agreement No. 653941.

References

1. E. Charkaluk A. Bignonnet, A. Constantinescu, K. Dang Van. Fatigue design of structures under thermomechanical loadings. Fatigue Fract Eng M **25** (2002): 1199-1206.
2. H. Sehitoglu. Thermal and thermomechanical fatigue of structural alloys. ASM International, Member/Customer Service Center, Materials Park, OH 44073-0002, USA (1996): 527-556.
3. A. Constantinescu, E. Charkaluk, G. Lederer, L. Verger. A computational approach to thermomechanical fatigue. Int J Fatigue, **26**, 8 (2004): 805-818.
4. R.W. Neu, H. Sehitoglu. Thermomechanical Fatigue, Oxidation and Creep: Part I. Damage Mechanisms. Metall Trans A, **20**, 9A (1989): 1755-1767.
5. R.W. Neu, H. Sehitoglu. Thermomechanical Fatigue, Oxidation and Creep: Part II. Life Prediction. Metall Trans A, **20**, 9 (1989): 1769-1783.
6. M. Nagode, M. Hack, M. Fajdiga. Low cycle thermo-mechanical fatigue: Damage operator approach. Fatigue Fract Eng M **33** (2009): 149-160.
7. M. Nagode, F. Längler, M. Hack. A time-dependent damage operator approach to thermo-mechanical fatigue of Ni-resist D-5S. Int J Fatigue, **33**, 5 (2011): 692-699.
8. K.N. Smith, P. Watson, T.H. Topper. A stress-strain function for the fatigue of metals. J Mater, JMLSA, **5,** 4 (1970): 767-778.
9. M. Nihei, P. Heuler, Ch. Boller, T. Seeger. Evaluation of mean stress effect on fatigue life by use of damage parameters. Int J Fatigue, **8**, 3 (1986): 119-126.
10. J.-L. Chaboche, Time-independent constitutive theories for cyclic plasticity, Int J Plasticity **2**, 2 (1986): 149-188.
11. J.-L. Chaboche, Constitutive equations for cyclic plasticity and cyclic viscoplasticity, Int J Plasticity **5**, 3 (1989): 247-302.
12. J. Papuga, M. Vargas, M. Hronek. Evaluation of uniaxial fatigue criteria applied to multiaxially

loaded unnotched samples. Engineer Mechan **19**, 2/3 (2012): 99-111.

13. M. Nagode, Continuous damage parameter calculation under thermomechanical random loading, MethodsX **1** (2014): 81-89.
14. M. Nesládek, J. Jurenka, M. Lutovinov, M. Růžička, P. Měšťánek, J. Džugan. An assessment of thermo-mechanically induced fatigue damage of a steam turbine shaft. Procedia Struct Integrity, **7** (2017): 190-197.